Atmos. Chem. Phys. Discuss., doi:10.5194/acp-2016-753, 2016
Manuscript under review for journal Atmos. Chem. Phys.
Published: 30 August 2016

Atmospheric Chemistry and Physics Discussions

Characterization of gas-phase organics using proton transfer reaction time-of-flight mass spectrometry: fresh and aged residential wood combustion emissions

Emily A. Bruns[a]*, Jay G. Slowik[a], Imad El Haddad[a], Dogushan Kilic[a], Felix Klein[a], Josef Dommen[a], Brice Temime-Roussel[b], Nicolas Marchand[b], Urs Baltensperger[a] and André S. H. Prévôt[a]*

[a]*Laboratory of Atmospheric Chemistry, Paul Scherrer Institute, 5232 Villigen, Switzerland*

[b]*Aix Marseille Université, CNRS, LCE UMR 7376, 13331, Marseille, France*

**Correspondence to:* E. A. Bruns (emily.bruns@psi.ch) or A. S. H. Prévôt (andre.prevot@psi.ch)

August 21, 2016

For submission to *Atmospheric Chemistry and Physics*

Atmos. Chem. Phys. Discuss., doi:10.5194/acp-2016-753, 2016
Manuscript under review for journal Atmos. Chem. Phys.
Published: 30 August 2016

Atmospheric Chemistry and Physics Discussions

Abstract

Organic gases emitted during the flaming phase of residential wood combustion are characterized individually and by functionality using proton transfer reaction time-of-flight mass spectrometry. The evolution of the organic gases is monitored during photochemical aging. Primary gaseous emissions are dominated by oxygenated species (e.g., acetic acid, acetaldehyde, phenol and methanol), many of which have deleterious health effects and play an important role in atmospheric processes such as secondary organic aerosol formation and ozone production. Residential wood combustion emissions differ considerably from open biomass burning in both absolute magnitude and relative composition. Ratios of acetonitrile, a potential biomass burning marker, to CO are considerably lower (~0.09 pptv $ppbv^{-1}$) than those observed in air masses influenced by open burning (~1-2 pptv $ppbv^{-1}$), which may make differentiation from background levels difficult, even in regions heavily impacted by residential wood burning. Considerable formic acid forms during aging (~200-600 mg kg^{-1} at an OH exposure of (4.5-5.5)×10^{7} molec cm^{-3} h), indicating residential wood combustion can be an important local source for this acid, the quantities of which are currently underestimated in models. Phthalic anhydride, a naphthalene oxidation product, is also formed in considerable quantities with aging (~55-75 mg kg^{-1} at an OH exposure of (4.5-5.5)×10^{7} molec cm^{-3} h). Although total NMOG emissions vary by up to a factor of ~9 between burns, SOA formation potential does not scale with total NMOG emissions and is similar in all experiments. This study is the first thorough characterization of both primary and aged organic gases from residential wood combustion and provides a benchmark for comparison of emissions generated under different burn parameters.

Atmos. Chem. Phys. Discuss., doi:10.5194/acp-2016-753, 2016
Manuscript under review for journal Atmos. Chem. Phys.
Published: 30 August 2016

Atmospheric Chemistry and Physics Discussions

1 Introduction

Residential wood combustion is a source of gaseous and particulate emissions in the atmosphere, including a complex mixture of non-methane organic gases (NMOGs) (McDonald et al., 2000; Schauer et al., 2001; Hedberg et al., 2002; Jordan and Seen, 2005; Pettersson et al., 2011; Evtyugina et al., 2014; Reda et al., 2015). NMOGs impact climate (Stocker et al., 2013) and health (Pouli et al., 2003; Bølling et al., 2009) both directly and through the formation of products during atmospheric processing (Mason et al., 2001; Kroll and Seinfeld, 2008; Shao et al., 2009), which makes NMOG characterization critical. Although two studies have speciated a large fraction of the NMOG mass emitted during residential wood combustion (McDonald et al., 2000; Schauer et al., 2001), these studies relied on offline chromatographic approaches, which are time consuming in terms of sample preparation and analysis and can introduce both positive and negative artifacts (Nozière et al., 2015). Relatively recently, the proton transfer reaction mass spectrometer (PTR-MS) has emerged as a powerful tool for online quantification of atmospherically-relevant NMOGs (Lindinger et al., 1998; Jordan et al., 2009) eliminating many of the artifacts associated with offline approaches. NMOGs emitted during open burning of a variety of biomass fuels in the laboratory have been recently quantified using a high resolution proton transfer reaction time-of-flight mass spectrometer (PTR-ToF-MS) (Stockwell et al., 2015) and select nominal masses were followed during aging of residential wood combustion emissions using a quadrupole PTR-MS (Grieshop et al., 2009a). However, a complete high-resolution characterization of residential wood combustion emissions has yet to be performed.

The quantities and composition of NMOGs emitted during residential wood combustion are highly dependent on a number of parameters including wood type, appliance type and burn conditions, and as few studies have characterized these NMOGs (McDonald et al., 2000; Schauer

Atmos. Chem. Phys. Discuss., doi:10.5194/acp-2016-753, 2016
Manuscript under review for journal Atmos. Chem. Phys.
Published: 30 August 2016

et al., 2001; Hedberg et al., 2002; Jordan and Seen, 2005; Pettersson et al., 2011; Evtyugina et al., 2014; Reda et al., 2015), further work is needed to constrain emission factors, as highlighted in the recent review article by Nozière et al. (2015). Also, little is known about the evolution of NMOGs from residential wood combustion with aging.

In this study, we present results from the first use of a smog chamber and a PTR-ToF-MS to characterize primary and aged gaseous emissions from residential wood combustion in real-time. This novel approach allows for an improved characterization of NMOG emissions, particularly oxygenated NMOGs, which are a considerable fraction of the total NMOG mass emitted during residential wood combustion (McDonald et al., 2000; Schauer et al., 2001). This study focuses on a narrow set of burn conditions, namely the flaming phase of beech wood combustion, in order to generate as reproducible emissions as possible for a complementary investigation of the effects of parameters such as temperature on the emissions. While these experiments are a narrow representation of real-world conditions, this novel work provides a benchmark and direction for future wood combustion studies.

2 Methods

2.1 Emission generation and smog chamber operation

Beech (*Fagus sylvatica*) logs are combusted in a residential wood burner (Avant, 2009, Attika) and emissions are sampled from the chimney through a heated line (473 K), diluted by a factor of ~8-10 using an ejector diluter (473 K, DI-1000, Dekati Ltd.) and injected into the smog chamber (~7 m^3) through a heated line (423 K). Emissions are sampled during the stable flaming phase of the burn and modified combustion efficiencies (MCEs), defined as the ratio between CO_2 and the sum of CO and CO_2, range from 0.974-0.978 (Table 1).

Atmos. Chem. Phys. Discuss., doi:10.5194/acp-2016-753, 2016
Manuscript under review for journal Atmos. Chem. Phys.
Published: 30 August 2016

Emissions are injected for 11-21 min and total dilution factors range from ~100-200. All experiments are conducted under similar conditions with starting wood masses in the burner of 2.9±0.3 kg and a wood moisture content of 19±2%. The smog chamber has an average temperature of 287.0±0.1 K and a relative humidity of 55±3% over all five experiments. After characterization of the primary emissions, as described below, a single dose of d9-butanol (2 µl, butanol-D9, 98%, Cambridge Isotope Laboratories) is injected into the chamber and a continuous injection of nitrous acid in air (2.3-2.6 l min^{-1}, ≥99.999%, Air Liquide) into the chamber begins. The decay of d9-butanol measured throughout aging is used to estimate hydroxyl radical (OH) exposures (Barmet et al., 2012). Nitrous acid produces OH upon irradiation in the chamber and is used to increase the degree of aging. Levels of NO_x in the chamber prior to aging range from ~150-350 ppb. The small continuous dilution in the chamber during aging due to the constant nitrous acid injection is accounted for using CO as an inert tracer. The chamber contents are irradiated with UV light (40 lights, 90-100 W, Cleo Performance, Philips) for 4.5-6 h (maximum OH exposures of (4.7-6.8)×10^7 molec cm^{-3} h which corresponds to ~2-3 days of aging in the atmosphere at an OH concentration of 1×10^6 molec cm^{-3}). Reported quantities of aged species are taken at OH exposures of (4.5-5.5)×10^7 (Table 1; ~1.9-2.3 days of aging in the atmosphere at an OH concentration of 1×10^6 molec cm^{-3}) (Barmet et al., 2012).

2.2 Gas-phase analysis

NMOGs with a proton affinity greater than that of water are measured using a PTR-ToF-MS (PTR-ToF-MS 8000, Ionicon Analytik GmbH) and CO_2, CO and CH_4 are measured using cavity ring-down spectroscopy (G2401, Picarro, Inc.). The PTR-ToF-MS operates with hydronium ion ($[H_2O+H]^+$) as the reagent, a drift tube pressure of 2.2 mbar, a drift tube voltage of 543 V and a drift tube temperature of 90°C leading to a ratio of the electric field (*E*) and the density of the

Atmos. Chem. Phys. Discuss., doi:10.5194/acp-2016-753, 2016
Manuscript under review for journal Atmos. Chem. Phys.
Published: 30 August 2016

105 buffer gas (*N*) in the drift tube (reduced electric field, *E*/*N*) of 137 Townsend (Td). The
106 transmission function is determined using a gas standard of six NMOGs of known concentration
107 (methanol, acetaldehyde, propan-2-one, toluene, *p*-xylene, 1,3,5-trimethylbenzene; Carbagas).
108 As the RH and temperature of the sampled air is similar in all experiments, changes in the
109 detection efficiency of individual species are not expected.

110 PTR-ToF-MS data are analyzed using the Tofware post-processing software (version 2.4.5,
111 TOFWERK AG, Thun, Switzerland; PTR module as distributed by Ionicon Analytik GmbH),
112 running in the Igor Pro 6.3 environment (version 6.3, Wavemetrics Inc.). The minimum
113 detection limit is taken as three standard deviations above the background, where the standard
114 deviation is determined from the measurements of each ion in the chamber prior to emission
115 injection. Isotopic contributions are constrained during peak fitting and are accounted for in
116 reported concentrations. Possible molecular formulas increase with increasing *m/z*, making
117 accurate peak assignments difficult in the higher *m/z* range. Mass spectral data from *m/z* 33 to
118 *m/z* 130 are assigned molecular formulas, as well as the ^{18}O isotope of the reagent ion and signal
119 above *m/z* 130 corresponding to compounds previously identified during residential wood
120 combustion (McDonald et al., 2000; Schauer et al., 2001; Hedberg et al., 2002; Jordan and Seen,
121 2005; Pettersson et al., 2011; Evtyugina et al., 2014; Reda et al., 2015). All signal above *m/z* 130
122 is included in total NMOG mass quantification. Using this approach, ~94-97% of the total
123 NMOG mass measured using the PTR-ToF-MS has an ion assignment.

124 The reaction rate constant of each species with the reagent ion in the drift tube is needed to
125 convert raw signal to concentration. When available, individual reaction rate constants are
126 applied to ions assigned a structure (Cappellin et al., 2012) (Table S1), otherwise a default
127 reaction rate constant of 2×10^{-9} cm^3 s^{-1} is applied. For possible isomers, the reaction rate

Atmos. Chem. Phys. Discuss., doi:10.5194/acp-2016-753, 2016
Manuscript under review for journal Atmos. Chem. Phys.
Published: 30 August 2016

Atmospheric Chemistry and Physics Discussions

constant is taken as the average of available values. Approximately 60-70% of the total NMOG mass is comprised of compounds with known rate constants. NMOG signal is normalized to $[H_2{}^{18}O+H]^+$ to convert to concentration. Emission factors (EFs) normalize concentrations to the total wood mass burned (e.g., mg kg^{-1} reads as mg of species emitted per kg wood burned) to facilitate comparison between experiments and are calculated as described previously (Andreae and Merlet, 2001; Bruns et al., 2015a).

PTR-ToF mass spectrometry is a relatively soft ionization technique generally resulting in protonation of the parent NMOG ($[M+H]^+$), although some compounds are known to produce other ions, for example through fragmentation or rearrangement (e.g., Baasandorj et al. (2015)). Reactions potentially leading to considerable formation of species besides $[M+H]^+$ are discussed in the Supplement. The extent to which reactions leading to ions other than $[M+H]^+$ occurs is dependent on instrument parameters such as *E*/*N*. The unknown relative contributions of various isomers makes it difficult to account for reactions generating ions besides $[M+H]^+$ and thus, no fragmentation corrections are applied. Emission factors of compounds likely to undergo extensive reaction to form products besides $[M+H]^+$ (i.e., methylcyclohexane (Midey et al., 2003), ethyl acetate (Baasandorj et al., 2015) and saturated aliphatic aldehydes (Buhr et al., 2002), with the exception of acetaldehyde) are not reported. Due to interferences, butenes ($[C_4H_8+H]^+$) are not quantified.

3 Results and Discussion

3.1 NMOG emissions

In all experiments, the largest EFs for a single gas-phase species correspond to CO_2 (1770-1790 g kg^{-1}) and CO (27-30 g kg^{-1}) (Table 2), which are in good agreement with previous

Atmos. Chem. Phys. Discuss., doi:10.5194/acp-2016-753, 2016
Manuscript under review for journal Atmos. Chem. Phys.
Published: 30 August 2016

Atmospheric Chemistry and Physics Discussions

measurements from residential beech logwood combustion where CO_2 EFs of ~1800 g kg^{-1} and CO EFs of ~20-70 g kg^{-1} were measured (Ozil et al., 2009; Schmidl et al., 2011; Kistler et al., 2012; Evtyugina et al., 2014; Reda et al., 2015). Methane is also emitted in considerable quantities (1.5-2.8 g kg^{-1}), similar to previously observed values for beech wood burning in fireplaces (0.5-1 g kg^{-1} (Ozil et al., 2009), however, at generally lower levels than total NMOGs (1.5-13 g kg^{-1}). Total NMOG EFs from beech wood combustion have not been previously reported, but values are similar to studies of residential wood stove burning of different hardwoods which have attempted a detailed quantification of total NMOGs, such as McDonald et al. (2000) (6.2-55.3 g kg^{-1} for a hardwood mixture) and Schauer et al. (2001) (6.7 g kg^{-1} for oak). Total NMOG quantities reported in this study refer to species quantified using the PTR-ToF-MS.

Although a large fraction of atmospherically-relevant organic gases are measured using the PTR-ToF-MS, some species are not quantitatively detected, including those with a proton affinity less than water (i.e., small alkanes). Based on previous studies of residential burning, alkanes are estimated to contribute less than ~5% to the NMOG mass of either hard or softwood and the sum of alkenes and alkynes, some of which are quantifiable with the PTR-ToF-MS, are estimated to contribute less than ~15% to the total measured NMOG mass (McDonald et al., 2000; Schauer et al., 2001).

Figure 1 shows the primary NMOG mass spectrum for each experiment classified by NMOG functionality and the fractional contribution of NMOG functional groups to the total NMOG mass. EFs for individual compounds are presented in Table 2. For ease of reading, nominal *m/z*s are presented in the text and figures, however, monoisotopic *m/z*s for all identified species can be found in Tables 2 and S2. Separation of isobaric species is possible using the PTR-ToF-MS,

Atmos. Chem. Phys. Discuss., doi:10.5194/acp-2016-753, 2016
Manuscript under review for journal Atmos. Chem. Phys.
Published: 30 August 2016

Atmospheric Chemistry and Physics Discussions

however, isomers remain indistinguishable. Quantities of gas-phase species generated during residential wood combustion depend on a variety of parameters, such as type of burner and wood species. However, many compounds are commonly emitted and structures are assigned to observed ions based on previously identified species (McDonald et al., 2000; Schauer et al., 2001; Hedberg et al., 2002; Jordan and Seen, 2005; Pettersson et al., 2011; Evtyugina et al., 2014; Reda et al., 2015). A few small, unambiguous ions are also assigned a structure, including methanol, formic acid and acetonitrile. Approximately 70% of the total NMOG mass measured using the PTR-ToF-MS is assigned a structure based on this method.

NMOGs are categorized by functional groups including: oxygenated, total C_xH_y, nitrogen-containing and other. Oxygenated subcategories include: acids (comprised of non-aromatic acids), carbonyls (comprised of non-aromatic carbonyls), oxygenated aromatics (not including furans), furans, O-containing (comprised of structurally unassigned oxygenated compounds and multifunctional oxygenated compounds) and O- and N-containing (comprised of species containing both oxygen and nitrogen atoms). Species categorized as N-containing contain no oxygen atoms. Total C_xH_y subcategories include: aromatic hydrocarbons, and non-aromatic and structurally unassigned species (referred to as C_xH_y in the text and figures). Higher molecular weight species lacking an ion assignment are categorized as "other". In the case of possible isomers, ions are categorized according to the species most likely to dominate based on previous studies (McDonald et al., 2000; Schauer et al., 2001; Hedberg et al., 2002; Jordan and Seen, 2005; Pettersson et al., 2011; Evtyugina et al., 2014; Reda et al., 2015).

Oxygenated species contribute ~68-94% to the total primary NMOG mass, which has important atmospheric implications due to the role of these compounds in photochemical reactions, for example by altering O_3 and peroxide formation (Mason et al., 2001; Shao et al., 2009).

Atmos. Chem. Phys. Discuss., doi:10.5194/acp-2016-753, 2016
Manuscript under review for journal Atmos. Chem. Phys.
Published: 30 August 2016

Atmospheric Chemistry and Physics Discussions

McDonald et al. (2000) and Schauer et al. (2001) previously observed the dominance of oxygenated NMOGs during residential burning of other wood types, whereas Evtyugina et al. (2014) found that benzene and benzene derivatives contributed 59% to the total measured NMOGs, compared to only 26% from oxygenated compounds for residential burning of beech wood in a woodstove. However, Evtyugina et al. (2014), as well as McDonald et al. (2000) and Schauer et al. (2001), did not include emissions from all lower molecular weight NMOGs, such as acetic acid. Oxygenated NMOGs are also reported as a large fraction of NMOGs emitted during open burning of many biomass fuels (Gilman et al., 2015; Stockwell et al., 2015).

Acids are the most abundant subclass of species in all experiments with an average EF of 2000±2000 mg kg^{-1} and acetic acid ($[C_2H_4O_2+H]^+$ at nominal *m/z* 61) is the most highly emitted compound in all experiments. In addition to acetic acid, $[C_2H_4O_2+H]^+$ can correspond to glycolaldehyde, however, Stockwell et al. (2015) found that acetic acid contributes ~75-93% to $[C_2H_4O_2+H]^+$ during open burning of black spruce (*Picea mariana)* and ponderosa pine (*Pinus ponderosa*) and thus, it is expected that this ion is also largely attributable to acetic acid in the current study. Acetic acid and formic acid ($[CH_2O_2+H]^+$ at nominal *m/z* 47) are the most abundant carboxylic acids in the atmosphere and are important contributors to atmospheric acidity (Chebbi and Carlier, 1996). However, the sources of these acids are poorly understood (Paulot et al., 2011) and data on their EFs from residential wood combustion are relatively unknown. The high acetic acid EFs found here indicate that residential wood combustion can be an important local source of this acid. Interestingly, the enhancement of acetic acid ($\Delta C_2H_4O_2$) over background levels relative to CO enhancement (ΔCO) in the current study ranges from ~6 to 80 pptv $ppbv^{-1}$ (Table 1), which is much higher than the average 0.58 pptv $ppbv^{-1}$ (sum of gas and aerosol phase) measured in an Alpine valley heavily impacted by residential wood

Atmos. Chem. Phys. Discuss., doi:10.5194/acp-2016-753, 2016
Manuscript under review for journal Atmos. Chem. Phys.
Published: 30 August 2016

Atmospheric Chemistry and Physics Discussions

combustion in winter (Gaeggeler et al., 2008). Further work is needed to investigate the source of this discrepancy, as limited ambient measurements are available from regions heavily impacted by residential wood combustion. However, it is possible that the ambient measurements were dominated by emissions produced during poor burning conditions (e.g., starting phase) where CO EFs are expected to be higher than during the stable burning phase investigated in the current study.

The sum of oxygenated and non-oxygenated aromatic compounds contribute ~7-30% (800±300 mg kg^{-1}) to the total primary NMOG mass with benzene ($[C_6H_6+H]^+$ at nominal *m/z* 79), phenol ($[C_6H_6O+H]^+$ at nominal *m/z* 95), and naphthalene ($[C_{10}H_8+H]^+$ at nominal *m/z* 129) as the three most dominant species. Oxidation products of aromatic species are the largest contributors to residential wood combustion SOA in this study (Bruns et al., 2016) and both aromatic and related oxidation products are of interest due to their particularly deleterious effects on health (Fu et al., 2012).

For the other functional group categories, carbonyl and alcohols contribute ~8-12% (600±600 mg kg^{-1}) and ~3-5% (300±300 mg kg^{-1}), respectively, to the total NMOG mass. In general, the most highly emitted carbonyl compound is acetaldehyde ($[C_2H_4O+H]^+$ at nominal *m/z* 45). Methanol ($[CH_3OH+H]^+$ at nominal *m/z* 33) is the most highly emitted alcohol, although other acyclic alcohols can undergo extensive fragmentation in the mass spectrometer. Furans are only a minor contributor to the total primary NMOG mass, contributing ~3-5% (300±300 mg kg^{-1}), but are of potential interest as several furans were recently identified as SOA precursors (Gómez Alvarez et al., 2009) and possible open biomass burning markers (Gilman et al., 2015).

3.2 Burn variability

Atmos. Chem. Phys. Discuss., doi:10.5194/acp-2016-753, 2016
Manuscript under review for journal Atmos. Chem. Phys.
Published: 30 August 2016

Atmospheric Chemistry and Physics Discussions

241 Although the same compounds are emitted during all burns, there is variability in EFs between
242 experiments despite efforts to replicate burns as closely as possible and the fact that the MCE for
243 each experiment falls within a narrow range (0.974-0.978) (Table 1). Experiments 2 and 3 show
244 marked differences in total NMOG EFs and NMOG composition compared to experiments 1, 4
245 and 5. For example, the total NMOG EF is ~9 times higher in experiment 2 compared to
246 experiment 5 (Table 2). Acetic acid EFs vary by a factor of ~15 between burns, with high
247 emissions in experiments 2 and 3 relative to experiments 1, 4 and 5. The total emission of
248 oxygenated species also correlates with acetic acid emissions, with total oxygenated EFs
249 considerably higher in experiments 2 and 3 than in experiments 1, 4 and 5. In contrast, aromatic
250 hydrocarbons and C_xH_y EFs show no correlation with total oxygenated species or acetic acid
251 EFs. Interestingly, differences in black carbon EFs, primary organic aerosol EFs and primary
252 organic aerosol mass to black carbon ratios are also not observed between these two groupings of
253 experiments (2, 3 and 1, 4, 5), as presented previously (Bruns et al., 2016). Enhancements in the
254 average EF for the different functional groups in experiments 2 and 3 relative to experiments 1, 4
255 and 5 are shown in Figure 2.

256 The differences in EFs due to inter-burn variability illustrate the difficulty in constraining EFs
257 from residential wood combustion. Further work to constrain the possible range of EFs
258 generated under different conditions is critical for improving model inputs. EFs are also
259 dependent on factors such as appliance type and fuel loading and further work is needed to
260 characterize the emissions and the evolution of these emissions with aging generated from
261 burning of different wood types and under different burn parameters.

262 **3.3 Biomass burning tracers**

Atmos. Chem. Phys. Discuss., doi:10.5194/acp-2016-753, 2016
Manuscript under review for journal Atmos. Chem. Phys.
Published: 30 August 2016

Atmospheric Chemistry and Physics Discussions

Individual compounds emitted exclusively or in large quantities during biomass burning are of interest for source apportionment and compounds contributing to SOA formation are of particular interest for climate and health (Figure 3). Acetonitrile is used as an ambient gas-phase marker for open biomass burning (de Gouw et al., 2003; Singh et al., 2003). In the current experiments, acetonitrile EFs are relatively low (3.5±0.3 mg kg^{-1}) compared to open biomass burning (~20-1000 mg kg^{-1}) (Yokelson et al., 2008; Yokelson et al., 2009; Akagi et al., 2013; Stockwell et al., 2015), likely due to different burn conditions (e.g., oxygen availability). The enhancements of acetonitrile over background levels relative to CO enhancement, $\Delta CH_3CN/\Delta CO$, are ~0.08-0.1 pptv $ppbv^{-1}$ (Table 1). This is slightly lower than the only previously published residential wood combustion measurements (0.1 to 0.8 pptv $ppbv^{-1}$) (Grieshop et al., 2009a), but is much lower than $\Delta CH_3CN/\Delta CO$ measurements in ambient air masses impacted by open biomass burning (~1-2 pptv $ppbv^{-1}$) (Holzinger et al., 1999; Andreae and Merlet, 2001; Christian et al., 2003; de Gouw et al., 2003; Jost et al., 2003; Holzinger et al., 2005; de Gouw et al., 2006; Warneke et al., 2006; Yokelson et al., 2008; de Gouw et al., 2009; Yokelson et al., 2009; Aiken et al., 2010; Akagi et al., 2013). However, $\Delta CH_3CN/\Delta CO$ during open burning has been shown to depend strongly on fuel type; Stockwell et al. (2015) observed $\Delta CH_3CN/\Delta CO$ values from 0.0060-7.1 pptv $ppbv^{-1}$ for individual open burns of different biomass types. Further work is needed to investigate CH_3CN emissions from residential burning of other wood types, as well as emissions during other burning phase (e.g., smoldering). However, these low enhancements may be difficult to differentiate from ambient background levels, making acetonitrile a poor marker for residential wood combustion.

The interference from isobaric compounds when quantifying acetonitrile using a PTR-MS is an important consideration when high resolution data are not available. Previously, several studies

Atmos. Chem. Phys. Discuss., doi:10.5194/acp-2016-753, 2016
Manuscript under review for journal Atmos. Chem. Phys.
Published: 30 August 2016

Atmospheric Chemistry and Physics Discussions

have determined this interference is minimal during open biomass burning (de Gouw et al., 2003; Warneke et al., 2003; Christian et al., 2004; Warneke et al., 2011). Recently, Dunne et al. (2012) quantified interferences with acetonitrile measurements in polluted urban air using a quadrupole PTR-MS and found contributions of 5-41% to *m/z* 42 from non-acetonitrile ions including: $[C_3H_6]^+$ and the ^{13}C isotope contribution from $[C_3H_5]^+$. In the current study, in addition to contributions from $[C_3H_6]^+$ and the isotopic contribution from $[C_3H_5]^+$, ~30-50% of the total signal at *m/z* 42 is due to $[C_2H_2O]^+$, which is presumably a fragment from higher molecular weight species. The total contribution to *m/z* 42 from species besides acetonitrile is ~70-85%. Although an investigation into the effects of the PTR-MS operating conditions (e.g., $[O_2]^+$ signal from ion source, *E*/*N* affecting fragmentation) is outside the scope of the current study, the possibility of considerable non-acetonitrile signal at *m/z* 42 should be taken into consideration when using nominal mass PTR-MS data to quantify acetonitrile from residential wood combustion.

Methanol is also used to identify air masses influenced by open biomass burning and enhancement over background levels relative to CO enhancement ($\Delta CH_3OH/\Delta CO$) is typically ~1-80 pptv $ppbv^{-1}$ in ambient and laboratory measurements of fresh open biomass burning emissions (Holzinger et al., 1999; Goode et al., 2000; Andreae and Merlet, 2001; Christian et al., 2003; Yokelson et al., 2003; Singh et al., 2004; Tabazadeh et al., 2004; Holzinger et al., 2005; de Gouw et al., 2006; Gaeggeler et al., 2008; Yokelson et al., 2008; Yokelson et al., 2009; Akagi et al., 2013; Stockwell et al., 2015; Müller et al., 2016). Here, we find similar values ranging from ~2-20 pptv $ppbv^{-1}$ (Table 1), in agreement with Gaeggeler et al. (2008) who measured a $\Delta CH_3OH/\Delta CO$ value of 2.16 pptv $ppbv^{-1}$ in an Alpine valley heavily impacted by residential wood combustion emissions in winter.

Atmos. Chem. Phys. Discuss., doi:10.5194/acp-2016-753, 2016
Manuscript under review for journal Atmos. Chem. Phys.
Published: 30 August 2016

Atmospheric Chemistry and Physics Discussions

3.4 Chamber studies of NMOG aging

Previous investigations of aged residential wood combustion emissions have largely focused on the evolution of the aerosol phase (Grieshop et al., 2009a; Grieshop et al., 2009b; Hennigan et al., 2010; Heringa et al., 2011; Bruns et al., 2015a; Bruns et al., 2015b; Bruns et al., 2016) and little is known about the evolution of the gas phase. The evolution of the NMOG functional group categories with increasing OH exposure is shown in Figure 4. Figure 5 shows the absolute change in mass spectral signal between the aged and primary NMOG quantities. Although an increase in NMOG mass could be expected with aging due to oxygenation, total NMOG mass decreases by ~5-30% at an OH exposure of (4.6-5.5)×10^7 molec cm^{-3} h relative to the primary emissions in experiments 1-4, likely due to the conversion of species from the gas to particle phase, the mass of which increased considerably with aging (Bruns et al., 2016), and the formation of gas-phase species not quantified here (e.g., formaldehyde). The total NMOG mass increases slightly, by ~5%, in experiment 5. Quantities of individual NMOGs and NMOG functional group categories after reaching an OH exposure of (4.6-5.5)×10^7 molec cm^{-3} h are presented in Table S2.

Subcategories of oxygenated species behave differently with aging. For example, total quantities (mg kg^{-1}) of oxygenated aromatic species decrease by factors of ~7-15 and furan quantities decrease by factors of ~4-9, whereas all other oxygenated subcategories, as well as N-containing species, remain within a factor of 2 of primary values at an OH exposure of (4.6-5.5)×10^7 molec cm^{-3} h. Aromatic hydrocarbons and C_xH_y quantities decrease with aging by factors of ~1.5-3. The large decreases in oxygenated aromatic species and furans illustrate the highly reactive nature of these species with respect to OH. The evolution of the bulk NMOG elemental composition during aging is shown in Figure S1 in the Supplement.

Atmos. Chem. Phys. Discuss., doi:10.5194/acp-2016-753, 2016
Manuscript under review for journal Atmos. Chem. Phys.
Published: 30 August 2016

Atmospheric Chemistry and Physics Discussions

In all experiments, formic acid quantities increases considerably with aging (by factors of ~5-50), as does $[C_4H_2O_3+H]^+$ at nominal *m/z* 99 (by factors of ~2-3), which likely corresponds to maleic anhydride, both of which are formed during the oxidation of aromatic species among other compounds (Bandow et al., 1985; Sato et al., 2007; Praplan et al., 2014). However, the fragment resulting from the loss of water from maleic acid cannot be distinguished from maleic anhydride using the PTR-ToF-MS. Formic acid is underestimated in models, likely due to missing secondary sources (Paulot et al., 2011) and these results indicate that aging of residential wood combustion emissions can result in considerable secondary formic acid production. The signal at *m/z* 149, corresponding to $[C_8H_4O_3+H]^+$, increases by factors of ~2-7 with aging. This ion likely corresponds to phthalic anhydride, which is a known naphthalene oxidation product (Chan et al., 2009).

Acetic acid formation has been observed in some ambient, open biomass burning plumes with aging (Goode et al., 2000; Hobbs et al., 2003; Yokelson et al., 2003), whereas not in others (de Gouw et al., 2006) and a doubling of *m/z* 61, likely dominated by acetic acid, was observed during aging of residential burning emissions in a previous laboratory study (Grieshop et al., 2009a). In the current study, no increase in the average acetic acid concentration relative to $CO_{(g)}$ is observed (Table 1). Note that this implies production of secondary acetic acid that compensates for the expected consumption of ~8-10% of primary acetic acid by reaction with OH at an OH exposure of $(4.5\text{-}5.5)\times10^7$ molec cm^{-3} h. These results indicate that acetic acid from residential burning of beech wood is dominated by primary emissions of this species (Table 1). As with acetic acid, there are discrepancies in methanol behavior as open biomass burning plumes undergo aging (Goode et al., 2000; Yokelson et al., 2003; Tabazadeh et al., 2004; Holzinger et al., 2005; de Gouw et al., 2006; Akagi et al., 2013). As described by Akagi et al.

Atmos. Chem. Phys. Discuss., doi:10.5194/acp-2016-753, 2016
Manuscript under review for journal Atmos. Chem. Phys.
Published: 30 August 2016

Atmospheric Chemistry and Physics Discussions

(2013), methanol enhancement has been hypothesized to correlate with terpene concentration and here, methanol remains within ~1-20% of the primary value after exposure to (4.5-5.5)×10^7 molec cm^{-3} h OH (Table 1), which is expected based on the reaction with OH (Overend and Paraskevopoulos, 1978) and the low terpene concentrations.

We have previously identified the compounds contributing to the majority of the SOA formed during these experiments (Bruns et al., 2016). Figure S2 shows the observed decay of the largest SOA precursors during aging in the chamber compared to the expected decay based on the OH concentration in the chamber and the reaction rate with respect to OH. There is good agreement between the observed and calculated decay for each compound which supports the structural assignment of each ion.

As described above, the overall primary emission profiles, as well as total NMOG emissions, vary considerably for experiments 2 and 3 compared to experiments 1, 4 and 5, with considerably higher total NMOG emissions in experiments 2 and 3. To determine the impact of the high NMOG emission experiments (2 and 3) compared to the lower NMOG emission experiments (1, 4 and 5) on SOA formation potential, individual SOA precursors with published SOA yields are investigated (Figure 3). The SOA formation potential for each of these 18 compounds is determined as the product of the primary EF and the best estimate SOA yield determined from the literature, as determined previously (Bruns et al., 2016). The total SOA formation potential for each experiment is taken as the sum of the individual SOA formation potentials. Interestingly, the SOA formation potential is similar in all experiments and the average enhancement of SOA formation potential in experiments 2 and 3 compared to the average of experiments 1, 4 and 5 is insignificant (Figure 2), despite the considerably different total NMOG EFs.

Atmos. Chem. Phys. Discuss., doi:10.5194/acp-2016-753, 2016
Manuscript under review for journal Atmos. Chem. Phys.
Published: 30 August 2016

Atmospheric Chemistry and Physics Discussions

4 Conclusions

This study is the first detailed characterization of primary NMOGs from residential wood combustion using a PTR-ToF-MS and the first investigation of the evolution of the majority of these NMOGs with aging. Differences in EFs and profiles between residential burning and open burning can be considerable and these results illustrate the importance of considering these emission sources individually. While total emissions from open burning are much larger than from residential burning, the societal relevance of residential wood burning emissions is nontrivial. A large fraction of open biomass burning derives from wildfires in sparsely populated regions (Ito and Penner, 2004), whereas residential wood combustion has been shown to be a major fraction of wintertime submicron organic aerosol in densely populated communities (Glasius et al., 2006; Krecl et al., 2008; Gonçalves et al., 2012; Guofeng et al., 2012; Crippa et al., 2013; Herich et al., 2014; Tao et al., 2014; Paraskevopoulou et al., 2015). Interestingly, MCE does not completely capture inter-burn variability, which is driven by differences in oxygenated content. This work clearly shows that measurements of total NMOGs or total hydrocarbon measurements are insufficient for estimating SOA formation potential from residential wood combustion. While this work characterizes the stable burning of beech wood in a modern woodstove, the composition and quantities of wood combustion emissions are highly dependent on many factors and further work is needed to characterize the emissions and the evolution of these emissions with aging generated from burning of different wood types and under different burn parameters.

Acknowledgements

399 The research leading to these results received funding from the European Community's Seventh
400 Framework Programme (FP7/2007-2013) under grant agreement no. 290605 (PSI-FELLOW),
401 from the Competence Center Environment and Sustainability (CCES) (project OPTIWARES)
402 and from the Swiss National Science Foundation (WOOSHI grant 140590 and starting grant
403 BSSGI0_155846). We are grateful to René Richter for technical assistance and to Mike Cubison
404 for analysis support.

405 **References**

406 Aiken, A.C., de Foy, B., Wiedinmyer, C., DeCarlo, P.F., Ulbrich, I.M., Wehrli, M.N., Szidat, S.,
407 Prevot, A.S.H., Noda, J., Wacker, L., Volkamer, R., Fortner, E., Wang, J., Laskin, A.,
408 Shutthanandan, V., Zheng, J., Zhang, R., Paredes-Miranda, G., Arnott, W.P., Molina, L.T., Sosa,
409 G., Querol, X. and Jimenez, J.L.: Mexico city aerosol analysis during MILAGRO using high
410 resolution aerosol mass spectrometry at the urban supersite (T0) – Part 2: Analysis of the
411 biomass burning contribution and the non-fossil carbon fraction, Atmos. Chem. Phys. 10, 5315-
412 5341, 2010.

413
414 Akagi, S.K., Yokelson, R.J., Burling, I.R., Meinardi, S., Simpson, I., Blake, D.R., McMeeking,
415 G.R., Sullivan, A., Lee, T., Kreidenweis, S., Urbanski, S., Reardon, J., Griffith, D.W.T.,
416 Johnson, T.J. and Weise, D.R.: Measurements of reactive trace gases and variable O_3 formation
417 rates in some South Carolina biomass burning plumes, Atmos. Chem. Phys. 13, 1141-1165,
418 2013.

419
420 Andreae, M.O. and Merlet, P.: Emission of trace gases and aerosols from biomass burning,
421 Global Biogeochem. Cy. 15, 955-966, 2001.

422
423 Baasandorj, M., Millet, D.B., Hu, L., Mitroo, D. and Williams, B.J.: Measuring acetic and formic
424 acid by proton-transfer-reaction mass spectrometry: sensitivity, humidity dependence, and
425 quantifying interferences, Atmos. Meas. Tech. 8, 1303-1321, 2015.

426
427 Bandow, H., Washida, N. and Akimoto, H.: Ring-cleavage reactions of aromatic hydrocarbons
428 studied by FT-IR spectroscopy. I. Photooxidation of toluene and benzene in the NO_x-Air System,
429 B. Chem. Soc. Jpn. 58, 2531-2540, 1985.

430
431 Barmet, P., Dommen, J., DeCarlo, P.F., Tritscher, T., Praplan, A.P., Platt, S.M., Prévôt, A.S.H.,
432 Donahue, N.M. and Baltensperger, U.: OH clock determination by proton transfer reaction mass
433 spectrometry at an environmental chamber, Atmos. Meas. Tech. 5, 647-656, 2012.

434
435 Bølling, A.K., Pagels, J., Yttri, K.E., Barregard, L., Sallsten, G., Schwarze, P.E. and Boman, C.:
436 Health effects of residential wood smoke particles: the importance of combustion conditions and
437 physicochemical particle properties, Part. Fibre Toxicol. 6, doi:10.1186/1743-8977-1186-1129,
438 2009.

439
440 Bruns, E.A., Krapf, M., Orasche, J., Huang, Y., Zimmermann, R., Drinovec, L., Močnik, G., El
441 Haddad, I., Slowik, J.G., Dommen, J., Baltensperger, U. and Prévôt, A.S.H.: Characterization of
442 primary and secondary wood combustion products generated under different burner loads,
443 Atmos. Chem. Phys. 15, 2825-2841, 2015a.

444
445 Bruns, E.A., El Haddad, I., Keller, A., Klein, F., Kumar, N.K., Pieber, S.M., Corbin, J.C.,
446 Slowik, J.G., Brune, W.H., Baltensperger, U. and Prévôt, A.S.H.: Inter-comparison of laboratory
447 smog chamber and flow reactor systems on organic aerosol yield and composition, Atmos. Meas.
448 Tech. 8, 2315-2332, 2015b.

449
450 Bruns, E.A., El Haddad, I., Slowik, J.G., Kilic, D., Klein, F., Baltensperger, U. and Prévôt,
451 A.S.H.: Identification of significant precursor gases of secondary organic aerosols from
452 residential wood combustion, Sci. Rep. 6, doi: 10.1038/srep27881, 2016.

453
454 Buhr, K., van Ruth, S. and Delahunty, C.: Analysis of volatile flavour compounds by Proton
455 Transfer Reaction-Mass Spectrometry: fragmentation patterns and discrimination between
456 isobaric and isomeric compounds, Int. J. Mass. Spectrom. 221, 1-7, 2002.

457
458 Cappellin, L., Karl, T., Probst, M., Ismailova, O., Winkler, P.M., Soukoulis, C., Aprea, E., Märk,
459 T.D., Gasperi, F. and Biasioli, F.: On quantitative determination of volatile organic compound
460 concentrations using proton transfer reaction time-of-flight mass spectrometry, Environ. Sci.
461 Technol. 46, 2283-2290, 2012.

462
463 Chan, A.W.H., Kautzman, K.E., Chhabra, P.S., Surratt, J.D., Chan, M.N., Crounse, J.D., Kürten,
464 A., Wennberg, P.O., Flagan, R.C. and Seinfeld, J.H.: Secondary organic aerosol formation from
465 photooxidation of naphthalene and alkylnaphthalenes: implications for oxidation of intermediate
466 volatility organic compounds (IVOCs), Atmos. Chem. Phys. 9, 3049-3060, 2009.

467
468 Chebbi, A. and Carlier, P.: Carboxylic acids in the troposphere, occurrence, sources, and sinks:
469 A review, Atmos. Environ. 30, 4233-4249, 1996.

470
471 Christian, T.J., Kleiss, B., Yokelson, R.J., Holzinger, R., Crutzen, P.J., Hao, W.M., Saharjo, B.H.
472 and Ward, D.E.: Comprehensive laboratory measurements of biomass-burning emissions: 1.
473 Emissions from Indonesian, African, and other fuels, J. Geophys. Res.-Atmos. 108,
474 doi:10.1029/2003JD003704, 2003.

475
476 Christian, T.J., Kleiss, B., Yokelson, R.J., Holzinger, R., Crutzen, P.J., Hao, W.M., Shirai, T. and
477 Blake, D.R.: Comprehensive laboratory measurements of biomass-burning emissions: 2. First
478 intercomparison of open-path FTIR, PTR-MS, and GC-MS/FID/ECD, J. Geophys. Res.-Atmos.
479 109, doi:10.1029/2003JD003874, 2004.

480
481 Crippa, M., DeCarlo, P.F., Slowik, J.G., Mohr, C., Heringa, M.F., Chirico, R., Poulain, L.,
482 Freutel, F., Sciare, J., Cozic, J., Di Marco, C.F., Elsasser, M., Nicolas, J.B., Marchand, N., Abidi,
483 E., Wiedensohler, A., Drewnick, F., Schneider, J., Borrmann, S., Nemitz, E., Zimmermann, R.,
484 Jaffrezo, J.L., Prévôt, A.S.H. and Baltensperger, U.: Wintertime aerosol chemical composition
485 and source apportionment of the organic fraction in the metropolitan area of Paris, Atmos. Chem.
486 Phys. 13, 961-981, 2013.

487
488 de Gouw, J.A., Warneke, C., Parrish, D.D., Holloway, J.S., Trainer, M. and Fehsenfeld, F.C.:
489 Emission sources and ocean uptake of acetonitrile (CH_3CN) in the atmosphere, J. Geophys. Res.-
490 Atmos. 108, doi:10.1029/2002JD002897, 2003.

491
492 de Gouw, J.A., Warneke, C., Stohl, A., Wollny, A.G., Brock, C.A., Cooper, O.R., Holloway,
493 J.S., Trainer, M., Fehsenfeld, F.C., Atlas, E.L., Donnelly, S.G., Stroud, V. and Lueb, A.: Volatile
494 organic compounds composition of merged and aged forest fire plumes from Alaska and western
495 Canada, J. Geophys. Res.-Atmos. 111, doi:10.1029/2005JD006175, 2006.

496
497 de Gouw, J.A., Welsh-Bon, D., Warneke, C., Kuster, W.C., Alexander, L., Baker, A.K.,
498 Beyersdorf, A.J., Blake, D.R., Canagaratna, M., Celada, A.T., Huey, L.G., Junkermann, W.,
499 Onasch, T.B., Salcido, A., Sjostedt, S.J., Sullivan, A.P., Tanner, D.J., Vargas, O., Weber, R.J.,
500 Worsnop, D.R., Yu, X.Y. and Zaveri, R.: Emission and chemistry of organic carbon in the gas
501 and aerosol phase at a sub-urban site near Mexico City in March 2006 during the MILAGRO
502 study, Atmos. Chem. Phys. 9, 3425-3442, 2009.

503
504 Dunne, E., Galbally, I.E., Lawson, S. and Patti, A.: Interference in the PTR-MS measurement of
505 acetonitrile at *m/z* 42 in polluted urban air—A study using switchable reagent ion PTR-MS, Int.
506 J. Mass. Spectrom. 319–320, 40-47, 2012.

507
508 Evtyugina, M., Alves, C., Calvo, A., Nunes, T., Tarelho, L., Duarte, M., Prozil, S.O., Evtuguin,
509 D.V. and Pio, C.: VOC emissions from residential combustion of Southern and mid-European
510 woods, Atmos. Environ. 83, 90-98, 2014.

511
512 Fu, P.P., Xia, Q., Sun, X. and Yu, H.: Phototoxicity and environmental transformation of
513 polycyclic aromatic hydrocarbons (PAHs)—light-induced reactive oxygen species, lipid
514 peroxidation, and DNA damage, J. Environ. Sci. Heal. C 30, 1-41, 2012.

515

516 Gaeggeler, K., Prevot, A.S.H., Dommen, J., Legreid, G., Reimann, S. and Baltensperger, U.:
517 Residential wood burning in an Alpine valley as a source for oxygenated volatile organic
518 compounds, hydrocarbons and organic acids, Atmos. Environ. 42, 8278-8287, 2008.

519
520 Gilman, J.B., Lerner, B.M., Kuster, W.C., Goldan, P.D., Warneke, C., Veres, P.R., Roberts, J.M.,
521 de Gouw, J.A., Burling, I.R. and Yokelson, R.J.: Biomass burning emissions and potential air
522 quality impacts of volatile organic compounds and other trace gases from fuels common in the
523 United States, Atmos. Chem. Phys. 15, 13915-13938, 2015.

524
525 Glasius, M., Ketzel, M., Wåhlin, P., Jensen, B., Mønster, J., Berkowicz, R. and Palmgren, F.:
526 Impact of wood combustion on particle levels in a residential area in Denmark, Atmos. Environ.
527 40, 7115-7124, 2006.

528
529 Gómez Alvarez, E., Borrás, E., Viidanoja, J. and Hjorth, J.: Unsaturated dicarbonyl products
530 from the OH-initiated photo-oxidation of furan, 2-methylfuran and 3-methylfuran, Atmos.
531 Environ. 43, 1603-1612, 2009.

532
533 Gonçalves, C., Alves, C. and Pio, C.: Inventory of fine particulate organic compound emissions
534 from residential wood combustion in Portugal, Atmos. Environ. 50, 297-306, 2012.

535
536 Goode, J.G., Yokelson, R.J., Ward, D.E., Susott, R.A., Babbitt, R.E., Davies, M.A. and Hao,
537 W.M.: Measurements of excess O_3, CO_2, CO, CH_4, C_2H_4, C_2H_2, HCN, NO, NH_3, HCOOH,
538 CH_3COOH, HCHO, and CH_3OH in 1997 Alaskan biomass burning plumes by airborne Fourier
539 transform infrared spectroscopy (AFTIR), J. Geophys. Res.-Atmos. 105, 22147-22166, 2000.

540
541 Grieshop, A.P., Logue, J.M., Donahue, N.M. and Robinson, A.L.: Laboratory investigation of
542 photochemical oxidation of organic aerosol from wood fires 1: measurement and simulation of
543 organic aerosol evolution, Atmos. Chem. Phys. 9, 1263-1277, 2009a.

544
545 Grieshop, A.P., Donahue, N.M. and Robinson, A.L.: Laboratory investigation of photochemical
546 oxidation of organic aerosol from wood fires 2: analysis of aerosol mass spectrometer data,
547 Atmos. Chem. Phys. 9, 2227-2240, 2009b.

548
549 Guofeng, S., Siye, W., Wen, W., Yanyan, Z., Yujia, M., Bin, W., Rong, W., Wei, L., Huizhong,
550 S., Ye, H., Yifeng, Y., Wei, W., Xilong, W., Xuejun, W. and Shu, T.: Emission factors, size
551 distributions, and emission inventories of carbonaceous particulate matter from residential wood
552 combustion in rural China, Environ. Sci. Technol. 46, 4207-4214, 2012.

553

554 Hedberg, E., Kristensson, A., Ohlsson, M., Johansson, C., Johansson, P.-Å., Swietlicki, E.,
555 Vesely, V., Wideqvist, U. and Westerholm, R.: Chemical and physical characterization of
556 emissions from birch wood combustion in a wood stove, Atmos. Environ. 36, 4823-4837, 2002.

557
558 Hennigan, C.J., Sullivan, A.P., Collett, J.L. and Robinson, A.L.: Levoglucosan stability in
559 biomass burning particles exposed to hydroxyl radicals, Geophys. Res. Lett. 37,
560 doi:10.1029/2010GL043088, 2010.

561
562 Herich, H., Gianini, M.F.D., Piot, C., Močnik, G., Jaffrezo, J.L., Besombes, J.L., Prévôt, A.S.H.
563 and Hueglin, C.: Overview of the impact of wood burning emissions on carbonaceous aerosols
564 and PM in large parts of the Alpine region, Atmos. Environ. 89, 64-75, 2014.

565
566 Heringa, M.F., DeCarlo, P.F., Chirico, R., Tritscher, T., Dommen, J., Weingartner, E., Richter,
567 R., Wehrle, G., Prévôt, A.S.H. and Baltensperger, U.: Investigations of primary and secondary
568 particulate matter of different wood combustion appliances with a high-resolution time-of-flight
569 aerosol mass spectrometer, Atmos. Chem. Phys. 11, 5945-5957, 2011.

570
571 Hobbs, P.V., Sinha, P., Yokelson, R.J., Christian, T.J., Blake, D.R., Gao, S., Kirchstetter, T.W.,
572 Novakov, T. and Pilewskie, P.: Evolution of gases and particles from a savanna fire in South
573 Africa, J. Geophys. Res.-Atmos. 108, doi:10.1029/2002JD002352, 2003.

574
575 Holzinger, R., Warneke, C., Hansel, A., Jordan, A., Lindinger, W., Scharffe, D.H., Schade, G.
576 and Crutzen, P.J.: Biomass burning as a source of formaldehyde, acetaldehyde, methanol,
577 acetone, acetonitrile, and hydrogen cyanide, Geophys. Res. Lett. 26, 1161-1164, 1999.

578
579 Holzinger, R., Williams, J., Salisbury, G., Klüpfel, T., de Reus, M., Traub, M., Crutzen, P.J. and
580 Lelieveld, J.: Oxygenated compounds in aged biomass burning plumes over the Eastern
581 Mediterranean: evidence for strong secondary production of methanol and acetone, Atmos.
582 Chem. Phys. 5, 39-46, 2005.

583
584 Ito, A. and Penner, J.E.: Global estimates of biomass burning emissions based on satellite
585 imagery for the year 2000, J. Geophys. Res.-Atmos. 109, doi:10.1029/2003JD004423, 2004.

586
587 Jordan, A., Haidacher, S., Hanel, G., Hartungen, E., Märk, L., Seehauser, H., Schottkowsky, R.,
588 Sulzer, P. and Märk, T.D.: A high resolution and high sensitivity proton-transfer-reaction time-
589 of-flight mass spectrometer (PTR-TOF-MS), Int. J. Mass. Spectrom. 286, 122-128, 2009.

590
591 Jordan, T.B. and Seen, A.J.: Effect of airflow setting on the organic composition of woodheater
592 emissions, Environ. Sci. Technol. 39, 3601-3610, 2005.

Jost, C., Trentmann, J., Sprung, D., Andreae, M.O., McQuaid, J.B. and Barjat, H.: Trace gas chemistry in a young biomass burning plume over Namibia: Observations and model simulations, J. Geophys. Res.-Atmos. 108, doi:10.1029/2002JD002431, 2003.

Kistler, M., Schmidl, C., Padouvas, E., Giebl, H., Lohninger, J., Ellinger, R., Bauer, H. and Puxbaum, H.: Odor, gaseous and PM_{10} emissions from small scale combustion of wood types indigenous to Central Europe, Atmos. Environ. 51, 86-93, 2012.

Krecl, P., Hedberg Larsson, E., Ström, J. and Johansson, C.: Contribution of residential wood combustion and other sources to hourly winter aerosol in Northern Sweden determined by positive matrix factorization, Atmos. Chem. Phys. 8, 3639-3653, 2008.

Kroll, J.H. and Seinfeld, J.H.: Chemistry of secondary organic aerosol: formation and evolution of low-volatility organics in the atmosphere, Atmos. Environ. 42, 3593-3624, 2008.

Lindinger, W., Hansel, A. and Jordan, A.: On-line monitoring of volatile organic compounds at pptv levels by means of proton-transfer-reaction mass spectrometry (PTR-MS) medical applications, food control and environmental research, Int. J. Mass. Spectrom. 173, 191-241, 1998.

Mason, S.A., Field, R.J., Yokelson, R.J., Kochivar, M.A., Tinsley, M.R., Ward, D.E. and Hao, W.M.: Complex effects arising in smoke plume simulations due to inclusion of direct emissions of oxygenated organic species from biomass combustion, J. Geophys. Res.-Atmos. 106, 12527-12539, 2001.

McDonald, J.D., Zielinska, B., Fujita, E.M., Sagebiel, J.C., Chow, J.C. and Watson, J.G.: Fine particle and gaseous emission rates from residential wood combustion, Environ. Sci. Technol. 34, 2080-2091, 2000.

Midey, A.J., Williams, S., Miller, T.M. and Viggiano, A.A.: Reactions of O_2^+, NO^+ and H_3O^+ with methylcyclohexane (C_7H_{14}) and cyclooctane (C_8H_{16}) from 298 to 700 K, Int. J. Mass. Spectrom. 222, 413-430, 2003.

Müller, M., Anderson, B.E., Beyersdorf, A.J., Crawford, J.H., Diskin, G.S., Eichler, P., Fried, A., Keutsch, F.N., Mikoviny, T., Thornhill, K.L., Walega, J.G., Weinheimer, A.J., Yang, M., Yokelson, R.J. and Wisthaler, A.: In situ measurements and modeling of reactive trace gases in a small biomass burning plume, Atmos. Chem. Phys. 16, 3813-3824, 2016.

632 Nozière, B., Kalberer, M., Claeys, M., Allan, J., D'Anna, B., Decesari, S., Finessi, E., Glasius,
633 M., Grgić, I., Hamilton, J.F., Hoffmann, T., Iinuma, Y., Jaoui, M., Kahnt, A., Kampf, C.J.,
634 Kourtchev, I., Maenhaut, W., Marsden, N., Saarikoski, S., Schnelle-Kreis, J., Surratt, J.D.,
635 Szidat, S., Szmigielski, R. and Wisthaler, A.: The molecular identification of organic compounds
636 in the atmosphere: state of the art and challenges, Chem. Rev. 115, 3919-3983, 2015.

637
638 Overend, R. and Paraskevopoulos, G.: Rates of hydroxyl radical reactions. 4. Reactions with
639 methanol, ethanol, 1-propanol, and 2-propanol at 296 K, J. Phys. Chem. 82, 1329-1333, 1978.

640
641 Ozil, F., Tschamber, V., Haas, F. and Trouvé, G.: Efficiency of catalytic processes for the
642 reduction of CO and VOC emissions from wood combustion in domestic fireplaces, Fuel
643 Process. Technol. 90, 1053-1061, 2009.

644
645 Paraskevopoulou, D., Liakakou, E., Gerasopoulos, E. and Mihalopoulos, N.: Sources of
646 atmospheric aerosol from long-term measurements (5 years) of chemical composition in Athens,
647 Greece, Sci. Total Environ. 527–528, 165-178, 2015.

648
649 Paulot, F., Wunch, D., Crounse, J.D., Toon, G.C., Millet, D.B., DeCarlo, P.F., Vigouroux, C.,
650 Deutscher, N.M., González Abad, G., Notholt, J., Warneke, T., Hannigan, J.W., Warneke, C., de
651 Gouw, J.A., Dunlea, E.J., De Mazière, M., Griffith, D.W.T., Bernath, P., Jimenez, J.L. and
652 Wennberg, P.O.: Importance of secondary sources in the atmospheric budgets of formic and
653 acetic acids, Atmos. Chem. Phys. 11, 1989-2013, 2011.

654
655 Pettersson, E., Boman, C., Westerholm, R., Boström, D. and Nordin, A.: Stove performance and
656 emission characteristics in residential wood log and pellet combustion, part 2: wood stove,
657 Energ. Fuel 25, 315-323, 2011.

658
659 Pouli, A.E., Hatzinikolaou, D.G., Piperi, C., Stavridou, A., Psallidopoulos, M.C. and Stavrides,
660 J.C.: The cytotoxic effect of volatile organic compounds of the gas phase of cigarette smoke on
661 lung epithelial cells, Free Radical Bio. Med. 34, 345-355, 2003.

662
663 Praplan, A.P., Hegyi-Gaeggeler, K., Barmet, P., Pfaffenberger, L., Dommen, J. and
664 Baltensperger, U.: Online measurements of water-soluble organic acids in the gas and aerosol
665 phase from the photooxidation of 1,3,5-trimethylbenzene, Atmos. Chem. Phys. 14, 8665-8677,
666 2014.

667
668 Reda, A.A., Czech, H., Schnelle-Kreis, J., Sippula, O., Orasche, J., Weggler, B., Abbaszade, G.,
669 Arteaga-Salas, J.M., Kortelainen, M., Tissari, J., Jokiniemi, J., Streibel, T. and Zimmermann, R.:
670 Analysis of gas-phase carbonyl compounds in emissions from modern wood combustion
671 appliances: influence of wood type and combustion appliance, Energ. Fuel 29, 3897-3907, 2015.

672
673 Sato, K., Hatakeyama, S. and Imamura, T.: Secondary organic aerosol formation during the
674 photooxidation of toluene: NO_x dependence of chemical composition, J. Phys. Chem. A 111,
675 9796-9808, 2007.

676
677 Schauer, J.J., Kleeman, M.J., Cass, G.R. and Simoneit, B.R.T.: Measurement of emissions from
678 air pollution sources. 3. C_1-C_{29} organic compounds from fireplace combustion of wood, Environ.
679 Sci. Technol. 35, 1716-1728, 2001.

680
681 Schmidl, C., Luisser, M., Padouvas, E., Lasselsberger, L., Rzaca, M., Ramirez-Santa Cruz, C.,
682 Handler, M., Peng, G., Bauer, H. and Puxbaum, H.: Particulate and gaseous emissions from
683 manually and automatically fired small scale combustion systems, Atmos. Environ. 45, 7443-
684 7454, 2011.

685
686 Shao, M., Lu, S., Liu, Y., Xie, X., Chang, C., Huang, S. and Chen, Z.: Volatile organic
687 compounds measured in summer in Beijing and their role in ground-level ozone formation, J.
688 Geophys. Res.-Atmos. 114, doi:10.1029/2008JD010863, 2009.

689
690 Singh, H.B., Salas, L., Herlth, D., Kolyer, R., Czech, E., Viezee, W., Li, Q., Jacob, D.J., Blake,
691 D., Sachse, G., Harward, C.N., Fuelberg, H., Kiley, C.M., Zhao, Y. and Kondo, Y.: In situ
692 measurements of HCN and CH_3CN over the Pacific Ocean: Sources, sinks, and budgets, J.
693 Geophys. Res.-Atmos. 108, doi:10.1029/2002JD003006, 2003.

694
695 Singh, H.B., Salas, L.J., Chatfield, R.B., Czech, E., Fried, A., Walega, J., Evans, M.J., Field,
696 B.D., Jacob, D.J., Blake, D., Heikes, B., Talbot, R., Sachse, G., Crawford, J.H., Avery, M.A.,
697 Sandholm, S. and Fuelberg, H.: Analysis of the atmospheric distribution, sources, and sinks of
698 oxygenated volatile organic chemicals based on measurements over the Pacific during TRACE-
699 P, J. Geophys. Res.-Atmos. 109, doi:10.1029/2003JD003883, 2004.

700
701 IPCC: Climate Change 2013: The Physical Science Basis. Contribution of Working Group I to
702 the Fifth Assessment Report of the Intergovernmental Panel on Climate Change, edited by:
703 Stocker, T.F., D. Qin, G.-K.P., M. Tignor, S. K. Allen, J. Boschung, A. Nauels, Y. Xia, V. Bex
704 and Midgley, P.M., Cambridge University Press, Cambridge, UK and New York, USA, 2013.

705
706 Stockwell, C.E., Veres, P.R., Williams, J. and Yokelson, R.J.: Characterization of biomass
707 burning emissions from cooking fires, peat, crop residue, and other fuels with high-resolution
708 proton-transfer-reaction time-of-flight mass spectrometry, Atmos. Chem. Phys. 15, 845-865,
709 2015.

710

711 Tabazadeh, A., Yokelson, R.J., Singh, H.B., Hobbs, P.V., Crawford, J.H. and Iraci, L.T.:
712 Heterogeneous chemistry involving methanol in tropospheric clouds, Geophys. Res. Lett. 31,
713 doi:10.1029/2003GL018775, 2004.

714
715 Tao, J., Gao, J., Zhang, L., Zhang, R., Che, H., Zhang, Z., Lin, Z., Jing, J., Cao, J. and Hsu, S.C.:
716 $PM_{2.5}$ pollution in a megacity of southwest China: source apportionment and implication, Atmos.
717 Chem. Phys. 14, 8679-8699, 2014.

718
719 Warneke, C., de Gouw, J.A., Kuster, W.C., Goldan, P.D. and Fall, R.: Validation of atmospheric
720 VOC measurements by proton-transfer-reaction mass spectrometry using a gas-chromatographic
721 preseparation method, Environ. Sci. Technol. 37, 2494-2501, 2003.

722
723 Warneke, C., de Gouw, J.A., Stohl, A., Cooper, O.R., Goldan, P.D., Kuster, W.C., Holloway,
724 J.S., Williams, E.J., Lerner, B.M., McKeen, S.A., Trainer, M., Fehsenfeld, F.C., Atlas, E.L.,
725 Donnelly, S.G., Stroud, V., Lueb, A. and Kato, S.: Biomass burning and anthropogenic sources
726 of CO over New England in the summer 2004, J. Geophys. Res.-Atmos. 111,
727 doi:10.1029/2005JD006878, 2006.

728
729 Warneke, C., Roberts, J.M., Veres, P., Gilman, J., Kuster, W.C., Burling, I., Yokelson, R. and de
730 Gouw, J.A.: VOC identification and inter-comparison from laboratory biomass burning using
731 PTR-MS and PIT-MS, Int. J. Mass. Spectrom. 303, 6-14, 2011.

732
733 Yokelson, R.J., Bertschi, I.T., Christian, T.J., Hobbs, P.V., Ward, D.E. and Hao, W.M.: Trace
734 gas measurements in nascent, aged, and cloud-processed smoke from African savanna fires by
735 airborne Fourier transform infrared spectroscopy (AFTIR), J. Geophys. Res.-Atmos. 108,
736 doi:10.1029/2002JD002322, 2003.

737
738 Yokelson, R.J., Christian, T.J., Karl, T.G. and Guenther, A.: The tropical forest and fire
739 emissions experiment: laboratory fire measurements and synthesis of campaign data, Atmos.
740 Chem. Phys. 8, 3509-3527, 2008.

741
742 Yokelson, R.J., Crounse, J.D., DeCarlo, P.F., Karl, T., Urbanski, S., Atlas, E., Campos, T.,
743 Shinozuka, Y., Kapustin, V., Clarke, A.D., Weinheimer, A., Knapp, D.J., Montzka, D.D.,
744 Holloway, J., Weibring, P., Flocke, F., Zheng, W., Toohey, D., Wennberg, P.O., Wiedinmyer,
745 C., Mauldin, L., Fried, A., Richter, D., Walega, J., Jimenez, J.L., Adachi, K., Buseck, P.R., Hall,
746 S.R. and Shetter, R.: Emissions from biomass burning in the Yucatan, Atmos. Chem. Phys. 9,
747 5785-5812, 2009.

748

749

Atmos. Chem. Phys. Discuss., doi:10.5194/acp-2016-753, 2016
Manuscript under review for journal Atmos. Chem. Phys.
Published: 30 August 2016

Atmospheric Chemistry and Physics Discussions

Table 1. Modified combustion efficiencies, OH exposures of reported aged values (molec cm^{-3} h) and enhancement of select species relative to CO enhancement above background levels (pptv $ppbv^{-1}$)

parameter	experiment					average[a]
	1	2	3	4	5	
MCE	0.975	0.978	0.977	0.974	0.978	0.976±0.002
OH exposure	4.5×10^7	5.5×10^7	5.3×10^7	5.2×10^7	4.7×10^7	-
$\Delta CH_3CN_{primary}/\Delta CO$	0.079	0.11	0.099	0.077	0.082	0.09±0.01
$\Delta CH_3CN_{aged}/\Delta CO$	0.084	0.11	0.11	0.072	0.069	0.09±0.02
$\Delta CH_3OH_{primary}/\Delta CO$	3.4	21	11	2.4	1.5	8±8
$\Delta CH_3OH_{aged}/\Delta CO$	3.4	19	11	2.5	1.8	7±7
$\Delta C_2H_4O_{2primary}/\Delta CO$	12	84	57	9.8	5.9	30±30
$\Delta C_2H_4O_{2aged}/\Delta CO$	12	68	48	9.4	6.5	30±30

[a]Uncertainties correspond to one sample standard deviation of the replicates.

Atmos. Chem. Phys. Discuss., doi:10.5194/acp-2016-753, 2016
Manuscript under review for journal Atmos. Chem. Phys.
Published: 30 August 2016

Atmospheric Chemistry and Physics Discussions

Table 2. Primary emission factors of gas-phase species (mg kg^{-1})[a,b]

species	monoisotopic *m/z*	structural assignment[c]	functional group	experiment 1	2	3	4	5	average[d]
CO_2				1780000	1781000	1777000	1772000	1784000	1779000 ±4000
CO				27000	26000	27000	30000	27000	28000±2000
CH_4				1800	1600	2000	2800	1500	1900±500
NMOG				2800	13000	9200	3200	1500	6000±5000
acid				750	5000	3500	700	340	2000±2000
O-containing				560	3400	2200	590	290	1000±1000
carbonyl				310	1500	960	270	170	600±600
oxygenated aromatic				230	780	520	270	140	400±300
alcohol				130	660	360	90	48	300±300
furan				93	680	410	95	51	300±300
O- and N-containing				120	81	77	120	91	100±20
C_xH_y				120	210	210	160	64	150±60
aromatic hydrocarbon				320	170	490	680	250	400±200
N-containing				20	39	36	23	16	30±10
other				140	390	310	160	94	200±100
$[CH_3OH+H]^+$	33.034	methanol	alcohol	110	660	360	87	47	300±300
$[C_2H_3N+H]^+$	42.034	acetonitrile	N-containing	3.4	3.4	4.1	3.6	3.2	3.5±0.3
$[C_3H_6+H]^+$	43.055	propene	C_xH_y	38	61	40	28	15	40±20
$[C_2H_4O+H]^+$	45.034	acetaldehyde	carbonyl	94	330	230	79	48	200±100
$[CH_2O_2+H]+$	47.013	formic acid	acid	9.9	96	100	31	4.2	50±50
$[C_2H_6O+H]^+$	47.050	ethanol	alcohol	16	BDL	3.3	2.5	BDL	4±7
$[C_4H_6+H]^+$	55.055	buta-1,3-diene	C_xH_y	14	38	33	14	5.7	20±10
$[C_3H_4O+H]^+$	57.034	prop-2-enal	carbonyl	45	160	120	45	25	80±60
$[C_2H_2O_2+H]^+$	59.013	oxaldehyde	carbonyl	BDL	BDL	BDL	1.3	BDL	0.3±0.6
$[C_3H_6O+H]^+$	59.050	propan-2-one propanal	carbonyl	54	190	120	30	30	80±70
$[C_2H_4O_2+H]^+$	61.029	acetic acid glycolaldehyde	acid	740	4900	3400	670	340	2000±2000
$[C_4H_4O+H]^+$	69.034	furan	furan	17	140	82	19	9.7	50±60
$[C_5H_8+H]^+$	69.070	isoprene cyclopentene	C_xH_y	3.4	12	9.4	2.8	1.1	3±2
$[C_4H_6O+H]^+$	71.050	(*E*)-but-2-enal 3-buten-2-one 2-methylprop-2-enal	carbonyl	25	120	72	19	14	50±40
$[C_5H_{10}+H]^+$	71.086	(*E*)-/(*Z*)-pent-2-ene 2-methylbut-1-ene 2-methylbut-2-ene pent-1-ene 3-methylbut-1-ene	C_xH_y	2.7	5.3	4.0	2.0	0.86	3±2
$[C_3H_4O_2+H]^+$	73.029	2-oxopropanal	carbonyl	26	140	96	26	15	60±50
$[C_4H_8O+H]^+$	73.065	butan-2-one butanal 2-methylpropanal	carbonyl	7.2	44	24	5.2	4.2	20±20
$[C_3H_6O_2+H]^+$	75.045	methyl acetate	O-containing	62	490	300	56	28	200±200
$[C_6H_6+H]^+$	79.055	benzene	aromatic hydrocarbon	210	90	300	450	150	200±100
$[C_5H_6O+H]^+$	83.050	2-methylfuran	furan	21	160	88	21	12	60±60
$[C_5H_8O+H]^+$	85.065	3-methyl-3-buten-2-one	carbonyl	10	69	39	8.7	5.4	30±30
$[C_6H_{12}+H]^+$	85.102	(*E*)-hex-2-ene 2-methyl-pent-2-ene	C_xH_y	BDL	2.2	1.6	0.60	BDL	1±1
$[C_4H_6O_2+H]^+$	87.045	butane-2,3-dione	carbonyl	51	450	250	52	26	200±200
$[C_7H_8+H]^+$	93.070	toluene	aromatic hydrocarbon	23	22	34	39	16	27±9
$[C_6H_6O+H]^+$	95.050	phenol	oxygenated aromatic	110	110	130	130	68	110±20
$[C_5H_4O_2+H]^+$	97.029	furan-2-carbaldehyde	furan	40	270	180	40	21	100±100
$[C_6H_8O+H]^+$	97.065	2,4-/2,5-dimethylfuran	furan	11	86	48	11	5.5	30±30
$[C_4H_2O_3+H]^+$	99.008	maleic anhydride[e]	O-containing	40	91	66	40	26	50±30
$[C_8H_8+H]^+$	105.070	styrene	aromatic hydrocarbon	12	8.0	20	24	9.6	15±7
$[C_7H_6O+H]^+$	107.050	benzaldehyde	oxygenated aromatic	18	14	23	27	11	18±7
$[C_8H_{10}+H]^+$	107.086	*m*-/*o*-/*p*-xylene ethylbenzene	aromatic hydrocarbon	4.2	6.9	7.5	6.3	2.9	6±2
$[C_7H_8O+H]^+$	109.065	*m*-/*o*-/*p*-cresol	oxygenated aromatic	24	71	48	25	14	40±20
$[C_6H_6O_2+H]^+$	111.045	*m*-/*o*-/*p*-benzenediol 2-methylfuraldehyde	oxygenated aromatic	26	150	86	22	14	60±50
$[C_9H_8+H]^+$	117.070	1*H*-indene	aromatic hydrocarbon	5.0	BDL	9.5	15	2.9	6±6
$[C_9H_{10}+H]^+$	119.086	2,3-dihydro-1*H*-indene	aromatic	2.3	2.8	3.9	3.3	1.3	3±1

Atmos. Chem. Phys. Discuss., doi:10.5194/acp-2016-753, 2016
Manuscript under review for journal Atmos. Chem. Phys.
Published: 30 August 2016

Atmospheric Chemistry and Physics Discussions

			hydrocarbon						
$[C_8H_8O+H]^+$	121.065	1-phenylethanone	oxygenated	8.3	14	13	8.8	4.6	10±4
		3-/4-methylbenzaldehyde	aromatic						
$[C_9H_{12}+H]^+$	121.102	*i*-propylbenzene	aromatic	1.0	2.4	2.3	1.2	0.68	1.5±0.8
		n-propylbenzene	hydrocarbon						
		1,3,5-trimethylbenzene							
$[C_8H_{10}O+H]^+$	123.081	2,4-/2,6-/3,5-dimethylphenol	oxygenated	4.7	36	18	4.9	3.0	10±10
			aromatic						
$[C_7H_8O_2+H]^+$	125.060	2-methoxyphenol	oxygenated	9.2	110	55	12	4.9	40±50
		methylbenzenediols	aromatic						
$[C_6H_6O_3+H]^+$	127.040	5-(hydroxymethyl)furan-2-carbaldehyde	furan	4.4	29	17	4.9	2.7	10±10
$[C_{10}H_8+H]^+$	129.070	naphthalene	aromatic	42	20	80	100	33	60±30
			hydrocarbon						
$[C_8H_{10}O_2+H]^+$	139.076	2-methoxy-4-methylphenol	oxygenated	3.2	59	29	6.2	1.8	20±20
		4-(2-hydroxyethyl)phenol	aromatic						
$[C_{11}H_{10}+H]^+$	143.086	1-/2-methylnaphthalene	aromatic	4.0	2.3	5.7	7.5	3.3	5±2
			hydrocarbon						
$[C_9H_6O_2+H]^+$	147.045	2,3-dihydroinden-1-one	oxygenated	11	13	13	11	6.0	11±3
			aromatic						
$[C_8H_4O_3+H]^+$	149.024	phthalic anhdyride[e]	O-containing	16	31	25	16	8.3	19±9
$[C_8H_8O_3+H]^+$	153.055	4-hydroxy-3-methoxybenzaldehyde	oxygenated	3.8	27	15	3.7	1.4	10±10
			aromatic						
$[C_{12}H_8+H]^+$	153.070	acenaphthylene	aromatic	6.1	3.6	12	15	8.3	9±5
			hydrocarbon						
$[C_9H_{12}O_2+H]^+$	153.092	4-ethyl-2-methoxyphenol	oxygenated	1.4	30	14	3.2	BDL	10±10
		1,2-dimethoxy-4-methylbenzene	aromatic						
$[C_8H_{10}O_3+H]^+$	155.071	2,6-dimethoxyphenol	oxygenated	2.2	73	35	7.8	1.0	20±30
			aromatic						
$[C_{12}H_{10}+H]^+$	155.086	1,1'-biphenyl	aromatic	3.1	BDL	4.3	6.1	2.9	3±2
		1,2-dihydroacenaphthylene	hydrocarbon						
$[C_{12}H_{12}+H]^+$	157.102	dimethylnaphthalene	aromatic	1.3	3.0	3.2	2.2	1.2	2.2±0.9
			hydrocarbon						
$[C_{10}H_{12}O_2+H]^+$	165.092	2-methoxy-4-[(*E*)-prop-1-enyl]phenol	oxygenated	0.92	24	13	2.3	0.59	8±10
		2-methoxy-4-prop-2-enylphenol	aromatic						
		2-methoxy-4-[(*Z*)-prop-1-enyl]phenol							
$[C_9H_{10}O_3+H]^+$	167.071	1-(4-hydroxy-3-methoxyphenyl)ethanone	oxygenated	2.5	11	6.7	2.2	1.2	5±4
		2,5-dimethylbenzaldehyde	aromatic						
		3,4-dimethoxybenzaldehyde							
$[C_{13}H_{10}+H]^+$	167.086	fluorene	aromatic	BDL	BDL	1.0	2.5	2.0	1±1
			hydrocarbon						
$[C_{10}H_{14}O_2+H]^+$)	167.107	2-methoxy-4-propylphenol	oxygenated	0.88	7.6	4.4	1.1	BDL	3±3
			aromatic						
$[C_9H_{12}O_3+H]^+$	169.086	2,6-dimethoxy-4-methylphenol	oxygenated	BDL	14	6.2	1.1	BDL	4±6
			aromatic						
$[C_{14}H_{10}+H]^+$	179.086	phenanthrene	aromatic	6.4	8.4	6.1	3.6	7.7	6±2
		anthracene	hydrocarbon						
$[C_{13}H_8O+H]^+$	181.065	fluoren-9-one	oxygenated	2.7	4.0	2.7	1.2	1.9	2±1
		phenalen-1-one	aromatic						
$[C_{10}H_{12}O_3+H]^+$	181.086	1-(4-hydroxy-3-methoxyphenyl)propan-2-one	oxygenated	BDL	4.2	2.6	1.1	0.69	2±2
			aromatic						
$[C_9H_{10}O_4+H]^+$	183.066	3,4-dimethoxybenzoic acid	oxygenated	1.1	BDL	1.4	1.1	1.0	0.9±0.5
		4-hydroxy-3,5-dimethoxybenzaldehyde	aromatic						
$[C_{10}H_{14}O_3+H]^+$	183.102	4-ethyl-2,6-dimethoxyphenol	oxygenated	1.0	7.4	4.2	1.0	BDL	3±3
			aromatic						
$[C_{15}H_{12}+H]^+$	193.102	1-/2-/3-/9-methylphenanthrene	aromatic	0.50	2.6	1.3	BDL	0.44	1±1
		2-methylanthracene	hydrocarbon						
$[C_{11}H_{14}O_3+H]^+$	195.102	1,3-dimethoxy-2-prop-2-enoxybenzene	oxygenated	BDL	1.7	1.2	BDL	BDL	0.6±0.8
		2,6-dimethoxy-4-[(*Z*)-prop-1-enyl]phenol	aromatic						
$[C_{16}H_{10}+H]^+$	203.086	fluoranthene	aromatic	BDL	0.87	BDL	BDL	BDL	0.2±0.4
		pyrene	hydrocarbon						
		acephenanthrylene							

[a]CO_2, CO and CH_4 are measured using cavity ring down spectroscopy and all other species are measured using the PTR-ToF-MS.
[b]BDL indicates value is below the detection limit.
[c]Multiple structural assignments for a given ion correspond to possible isomers.
[d]Uncertainties correspond to one sample standard deviation of the replicates.
[e]Structural assignment based on known products produced during oxidation of aromatics (Bandow et al., 1985; Chan et al., 2009; Praplan et al., 2014).

Atmos. Chem. Phys. Discuss., doi:10.5194/acp-2016-753, 2016
Manuscript under review for journal Atmos. Chem. Phys.
Published: 30 August 2016

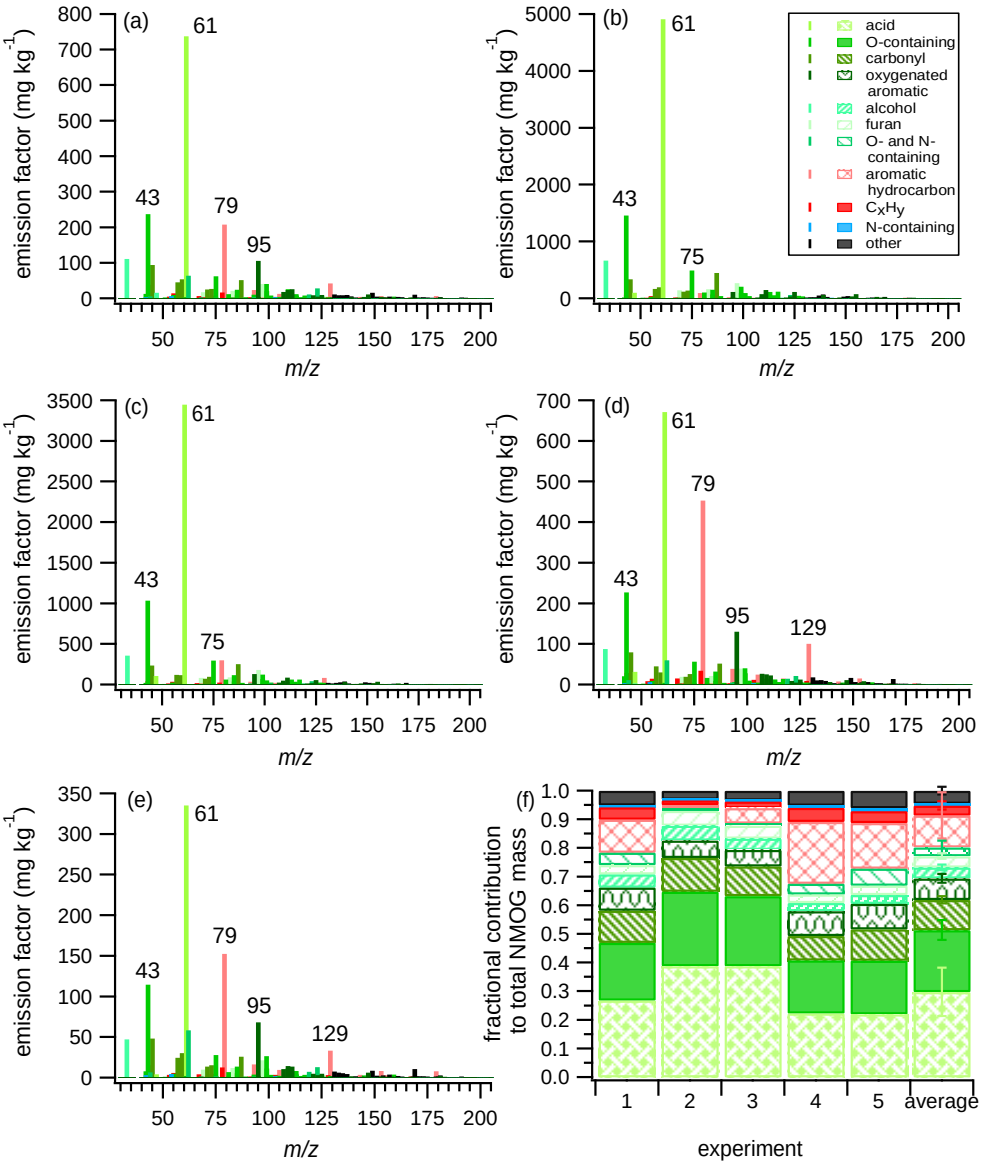

Figure 1. Mass spectra of primary emissions for experiments 1-5 (a-e) colored by functional group. (a-e) Labelled peaks correspond to $[C_2H_3O]^+$ (*m/z* 43, fragment from higher molecular weight compounds), $[C_2H_4O_2+H]^+$ (*m/z* 61, acetic acid), $[C_3H_6O_2+H]^+$ (*m/z* 75, methyl acetate), $[C_6H_6+H]^+$ (*m/z* 79, benzene), $[C_6H_6O+H]^+$ (*m/z* 95, phenol) and $[C_{10}H_8+H]^+$ (*m/z* 129, naphthalene). The bars in (f) correspond to the fractional contribution of each functional group to the total NMOG mass for each experiment and the average of all experiments. Error bars correspond to one sample standard deviation of the replicates. Legend in (b) applies to (a-f).

Atmos. Chem. Phys. Discuss., doi:10.5194/acp-2016-753, 2016
Manuscript under review for journal Atmos. Chem. Phys.
Published: 30 August 2016

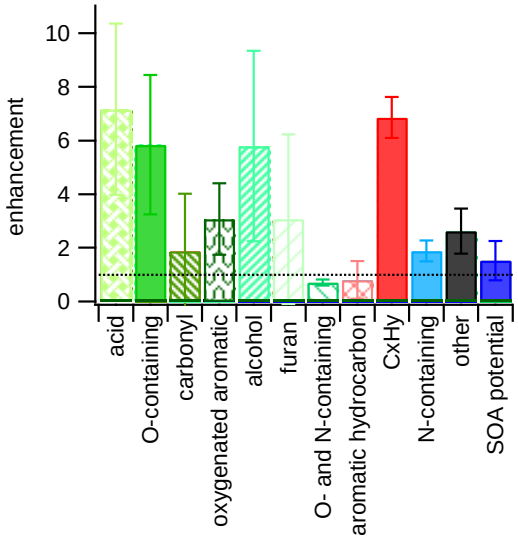

Figure 2. Enhancement (average value (mg kg^{-1}) of experiments 2 and 3 relative to the average value of experiments 1, 4 and 5) in each NMOG functional group category and for SOA formation potential. Total SOA formation potential is determined using the primary EF of each NMOG identified as a SOA precursor and literature SOA yields and assumes complete consumption of each NMOG with aging (see text for details). Error bars correspond to one sample standard deviation.

Atmos. Chem. Phys. Discuss., doi:10.5194/acp-2016-753, 2016
Manuscript under review for journal Atmos. Chem. Phys.
Published: 30 August 2016

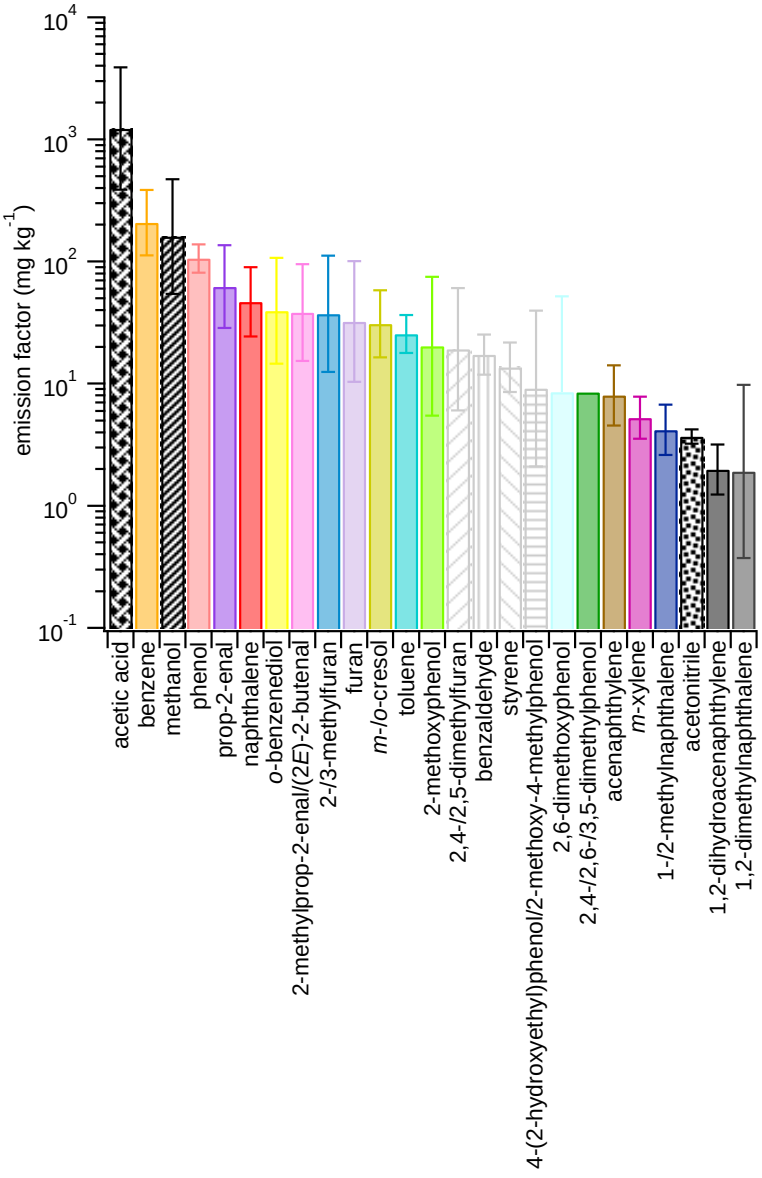

Figure 3. Geometric mean of the primary emission factors for gas-phase species of particular interest for SOA formation (solid bars and gray patterned bars) and identification of air masses influenced by biomass burning (black patterned bars). Colors and patterns corresponding to NMOGs contributing to SOA formation are consistent with Bruns et al. (2016). Error bars correspond to the sample geometric standard deviation of the replicates.

Atmos. Chem. Phys. Discuss., doi:10.5194/acp-2016-753, 2016
Manuscript under review for journal Atmos. Chem. Phys.
Published: 30 August 2016

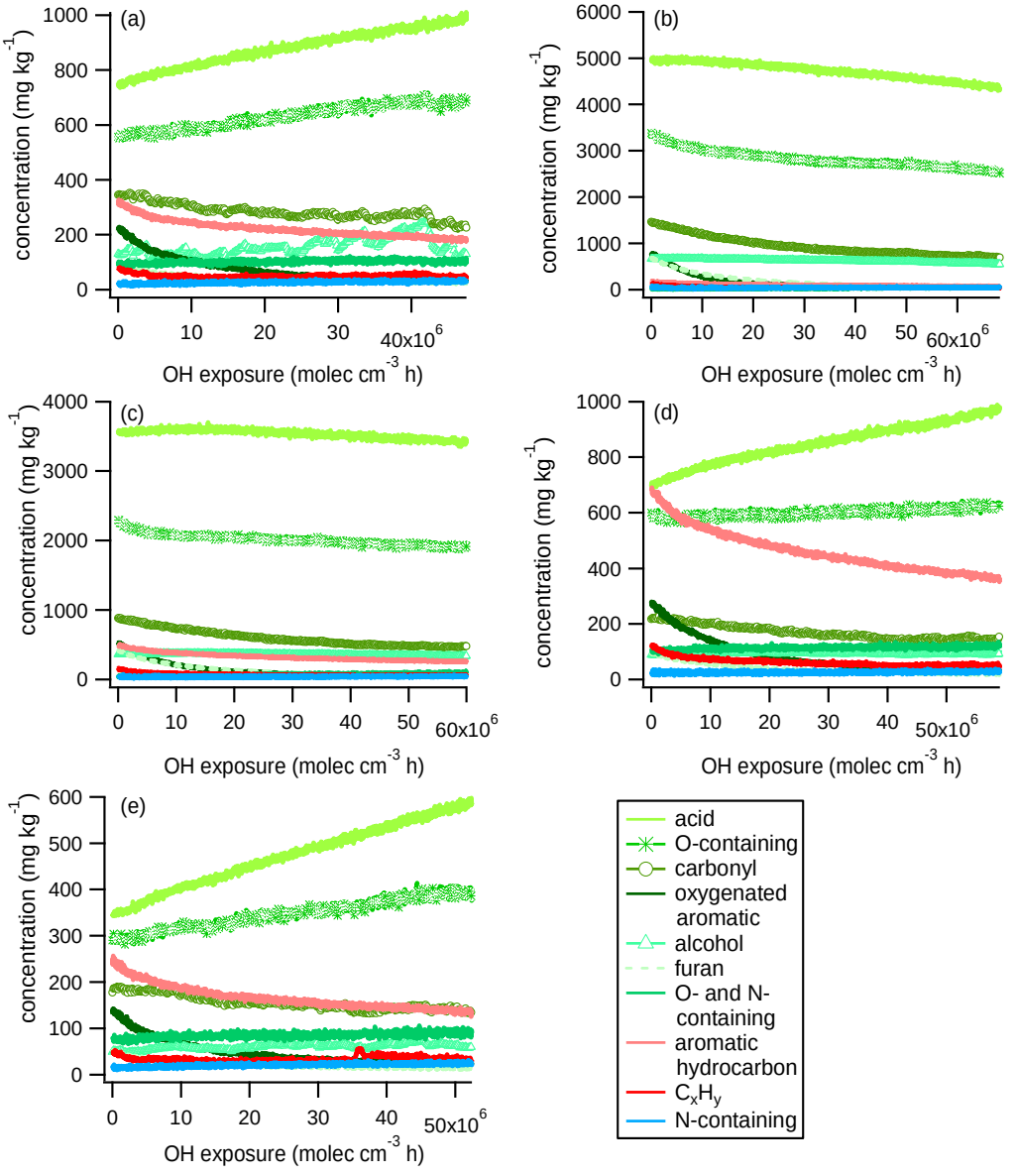

Figure 4. (a-e) Temporal evolution of gas-phase species categorized by functional group throughout aging in the smog chamber. Units on the y-axes are mass of each functional group (mg) per mass of wood consumed (kg).

Atmos. Chem. Phys. Discuss., doi:10.5194/acp-2016-753, 2016
Manuscript under review for journal Atmos. Chem. Phys.
Published: 30 August 2016

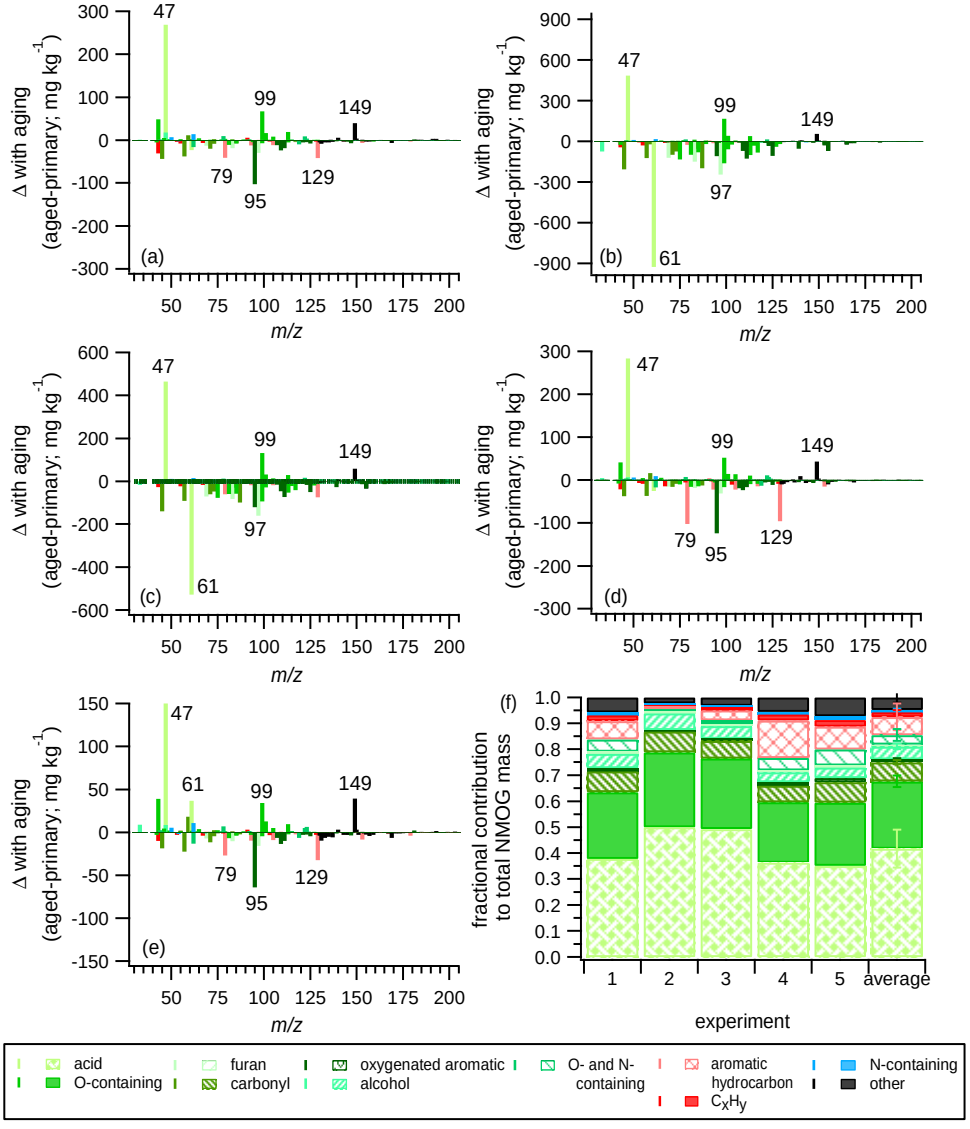

Figure 5. Absolute difference of aged and primary mass spectra for experiments 1-5 (a-e), where peaks less than zero decrease during aging and peaks greater than zero increase during aging. Aged emissions correspond to an OH exposure of (4.5-5.5)×10^7 molec cm^{-3} h. (a-e) Labelled peaks correspond to $[CH_2O_2+H]^+$ (*m/z* 47, formic acid), $[C_2H_4O_2+H]^+$ (*m/z* 61, acetic acid), $[C_6H_6+H]^+$ (*m/z* 79, benzene), $[C_6H_6O+H]^+$ (*m/z* 95, phenol), $[C_5H_4O_2+H]^+$ (*m/z* 97, furan-2-carbaldehyde), $[C_4H_2O_3+H]^+$ (*m/z* 99, maleic anhydride), $[C_{10}H_8+H]^+$ (*m/z* 129, naphthalene) and $[C_8H_4O_3+H]^+$ (*m/z* 149, phthalic anhydride). The bars in (f) correspond to the fractional contribution of each category to the total NMOG EF at an OH exposure of (4.5-5.5)×10^7 molec cm^{-3} h for each experiment and the average of all experiments. Error bars correspond to one sample standard deviation of the replicates.